

Isotopomer Selective Spectroscopy on Pentacene

Jürgen Köhler,* Albert-Jan C. Brouwer, Edgar J. J. Groenen, and Jan Schmidt

Contribution from the Centre for the Study of Excited States of Molecules, Huygens Laboratory, Leiden University, P.O. Box 9504, 2300 RA Leiden, The Netherlands

Received September 9, 1997. Revised Manuscript Received December 8, 1997

Abstract: By combining the selectivity of high-resolution laser spectroscopy with the specificity of hyperfine interactions in zero-field magnetic-resonance spectroscopy, ^{13}C -containing isotopomers of pentacene have been observed in natural-abundance samples and ^1H -containing isotopomers of pentacene in “fully” deuterated samples. Molecules containing two ^{13}C nuclei or up to four residual ^1H nuclei have been identified.

Introduction

Isotopically labeled molecules are being used in various fields of spectroscopy to obtain structural information. Different isotopes have different atomic masses and the replacement of one isotope by another produces a change in the rotational and vibrational frequencies. Such substitutions are successfully applied to interpret the microwave, infrared/Raman and optical spectra of molecules.¹ Some isotopes have a nuclear magnetic moment and are being used in magnetic-resonance spectroscopy.² Most frequent labels in organic chemistry are ^2H and ^{13}C , both having a nuclear magnetic moment while the most abundant carbon isotope ^{12}C has none. Often the spectroscopist can start working only after a sophisticated, time-consuming and expensive chemical synthesis of molecules isotopically labeled at specific positions. However, isotopically substituted molecules are present in natural abundance samples and a low abundance of a certain isotope need not be prohibitive. For example, for an organic molecule with 20 carbon nuclei about one in every five molecules contains a ^{13}C nucleus even though the natural abundance of ^{13}C is only 1.1%. An analogous conclusion can be drawn with respect to “completely” isotopically substituted molecules, e.g. perdeuterated ones. In the synthesis the substitution will likely remain incomplete for some molecules and spectroscopy may be performed on those molecules in otherwise completely substituted samples. The latter possibility would confine the chemical synthesis to a full isotopic substitution instead of more difficult selective ones. The success of such an approach, the spectroscopic study of a specific isotopomer in a natural abundance or fully labeled sample, obviously depends on the selectivity and sensitivity of the spectroscopic technique.

For UV/vis spectroscopy the possibility to identify a specific isotopomer relies on the fact that the frequency of an electronic transition depends on the isotopic constitution of the molecule. In Figure 1, the energy level diagram of a typical organic dye molecule is shown. Between the two singlet states S_1 and S_0 the transition, marked ① in Figure 1, is electric-dipole allowed and shows up as a so-called zero-phonon line in the absorption spectrum. The name refers to the fact that no vibrational excitations of the molecule are involved in the transition.

(1) Herzberg, G. *Molecular Spectra and Molecular Structure. II. Infrared and Raman Spectra of Polyatomic Molecules*; D. van Nostrand Company, Inc.: Princeton, 1966.

(2) Günther, H. *NMR spectroscopy. An Introduction*; John Wiley & Sons: New York, 1990.

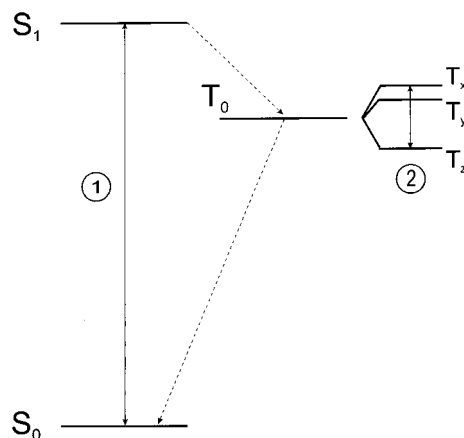


Figure 1. Schematic representation of the energy level scheme for a typical organic dye molecule. S_0 denotes the singlet ground state and S_1 the lowest excited singlet state. T_0 is the lowest triplet state. In general the degeneracy of the triplet sublevels, T_x , T_y , and T_z , is lifted by the magnetic dipole–dipole interaction of the two unpaired electrons. The arrows labeled ① and ② indicate the electric-dipole transition between S_1 and S_0 and a magnetic-dipole transition between two triplet sublevels, respectively. The dashed arrows indicate radiationless transitions.

Nevertheless, vibrations exert a small influence on the $S_1 \leftarrow S_0$ transition energy owing to the zero-point vibrational energy of the molecule. Consequently, the transition energy carries information about the molecular vibrational frequencies which in turn depend on the vibrating masses and thus on the isotopic composition. The $S_1 \leftarrow S_0$ zero-phonon line splits up in several components, corresponding to isotopically different molecules, which, depending on the line width, may be observed by means of optical spectroscopy. Depending on the total weight of the molecule, the specific position of the different isotopes, and their relative mass difference, the separation of the spectral components is on the order of $0.1\text{--}3\text{ cm}^{-1}$ whereas the transition energy is about $15000\text{--}30000\text{ cm}^{-1}$.

Besides the singlet states S_0 and S_1 in Figure 1, a triplet state T_0 exists which has two unpaired electrons and consequently a total electron spin angular momentum $S = 1$. Transitions from S_0 to T_0 are commonly forbidden by spin selection rules. The triplet state is populated by intersystem crossing from an excited singlet state, typically S_1 . The triplet state has three sublevels, T_x , T_y , and T_z , which are in general not degenerate even in the absence of an external magnetic field, because of the magnetic

dipole–dipole interaction between the unpaired electrons.³ Magnetic dipole transitions can be induced between the triplet sublevels by resonant microwaves, as indicated by the label ② in Figure 1. The line shape of such magnetic-resonance transitions depends on the nuclear composition of the molecule owing to the hyperfine interaction of the triplet electron spin with the surrounding nuclear magnetic moments.⁴ Because different nuclei carry different magnetic moments and the triplet electron-spin density varies with the position in the molecule, each nucleus will contribute to the line width depending on its character and position in the molecule. In other words, the triplet magnetic-resonance transition of a particular isotopomer will have a characteristic line shape that might allow its identification.

In fluorescence-detected-magnetic-resonance (FDMR) spectroscopy⁵ both aforementioned techniques are combined. For this double-resonance experiment, the sample is simultaneously illuminated with light to induce the $S_1 \leftarrow S_0$ transition and by microwaves to induce a transition between two triplet sublevels. The occurrence of a resonance in the triplet manifold is recorded as a change in the fluorescence intensity. Tuning a narrow-band laser into resonance with a distinct component of the isotopically split zero-phonon line allows only those isotopomers that absorb at this frequency to contribute to the fluorescence and therefore to the magnetic-resonance signal. The optical part of the experiment enables the selection of molecules with a particular isotopic composition while the magnetic-resonance part contributes to their identification.

The practical problem to observe an absorption line accompanied by one or several weak isotopic satellites results from a phenomenon called inhomogeneous line broadening. For a single molecule at low temperatures, the spectral width of the $S_1 \leftarrow S_0$ absorption line is determined by the lifetime of the S_1 state, typically about 10 ns, which corresponds to a homogeneous line width of 15 MHz (0.0005 cm^{-1}). For an ensemble of molecules, each one may experience a slightly different local environment, which leads to a distribution of transition energies—the inhomogeneous line width. For chromophores embedded in a disordered matrix, like a glass, the inhomogeneous line width commonly amounts to $100\text{--}1000 \text{ cm}^{-1}$, which reduces to a few wavenumbers for a single (host) crystal. Typically the ratio of the inhomogeneous-to-homogeneous line width is on the order of $10^4\text{--}10^5$, sufficient to bury the weaker isotopic features somewhere in the inhomogeneously broadened absorption profile.

In this contribution we illustrate the observation and identification of specific isotopomers in a sample of pentacene ($\text{C}_{22}\text{H}_{14}$) doped into a *p*-terphenyl ($\text{C}_{18}\text{H}_{14}$) host crystal. By combining careful crystal preparation and high detection sensitivity it proved possible to select a highly ordered crystal volume featuring an inhomogeneous line width which is narrow enough to resolve the satellite absorption lines of isotopically substituted molecules. This enabled us to study ^{13}C -containing molecules in natural abundance samples and ^1H -containing molecules in “completely” deuterated samples.

Results

In Figure 2, part of the fluorescence-excitation spectra of pentacene- h_{14} in *p*-terphenyl- h_{14} (Figure 2a) and of pentacene-

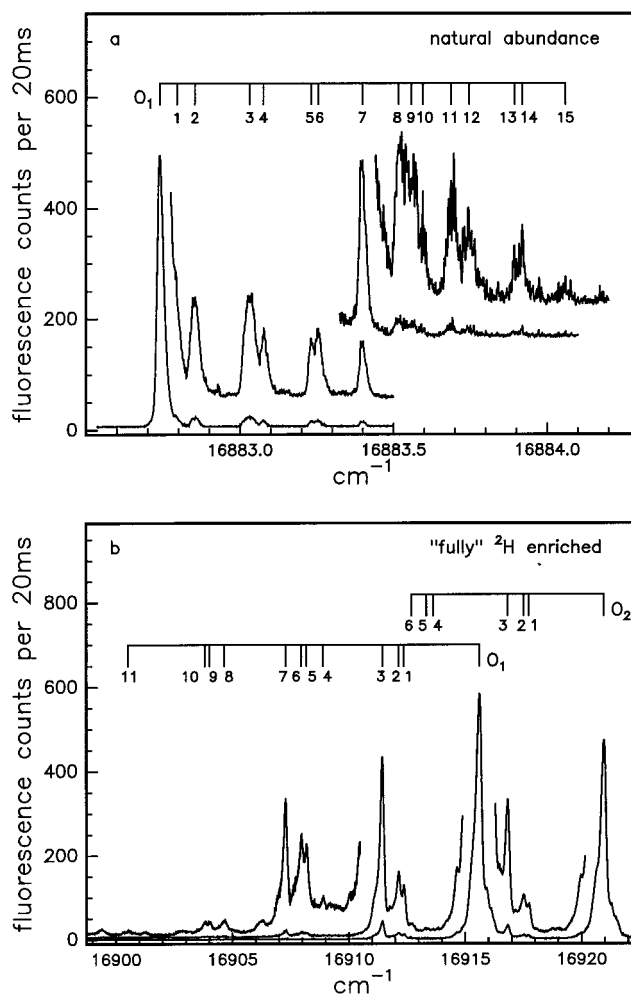


Figure 2. (a) Fluorescence-excitation spectrum of the O_1 spectral region of natural abundance pentacene in *p*-terphenyl at 1.2 K. (b) Fluorescence-excitation spectrum of the O_1/O_2 spectral region for “fully” ^2H enriched pentacene in *p*-terphenyl- d_{14} at 1.2 K. For both spectra the intensity scale is valid for the lowest trace. The other traces have been enlarged and offset for clarity.

d_{14} in *p*-terphenyl- d_{14} (Figure 2b) are shown. Both spectra reveal a complex pattern of lines. For the mixed crystal, each pentacene molecule replaces one *p*-terphenyl molecule substitutionally. At low temperatures the *p*-terphenyl host crystal has four different crystal sites leading to four spectral origins in the pentacene absorption spectrum, known as O_1 to O_4 .⁶

The top spectrum in Figure 2 has been recorded for a natural abundance sample and corresponds to the O_1 origin of the pentacene absorption. The most intense absorption occurs at $16\,882.739 \text{ cm}^{-1}$ and has a line width of only 0.025 cm^{-1} (750 MHz). Toward higher energy a set of satellites is observed, labeled 1–7. Satellite 1 appears as a weak shoulder in the wing of the main line. Satellites 2 and 7 show simple line shapes while bands between show structure. Further to the blue an additional set of even weaker bands is present, labeled 8–15 in Figure 2a.

For the lower spectrum a sample has been used that was 99% ^2H enriched. Its fluorescence-excitation spectrum is even more complex. At positions $16\,915.629$ and $16\,920.965 \text{ cm}^{-1}$, two zero-phonon lines corresponding to the O_1 and O_2 origins are observed. Apart from these two lines a whole series of satellites is present in the spectrum. The connected bars above the

(3) McGlynn, S. P.; Azumi, T.; Kinoshita, M. *Molecular spectroscopy of the triplet state*; Prentice Hall: Englewood, 1969.

(4) Schmidt, J.; van der Waals, J. H. *Chem. Phys. Lett.* **1969**, *3*, 546–549.

(5) Clarke, R. H. *Triplet State ODMR Spectroscopy*; Wiley & Sons: New York, 1982.

(6) Marchetti, A. P.; McColgin, W. C.; Eberly, J. H. *Phys. Rev. Lett.* **1975**, *35*, 387–390.

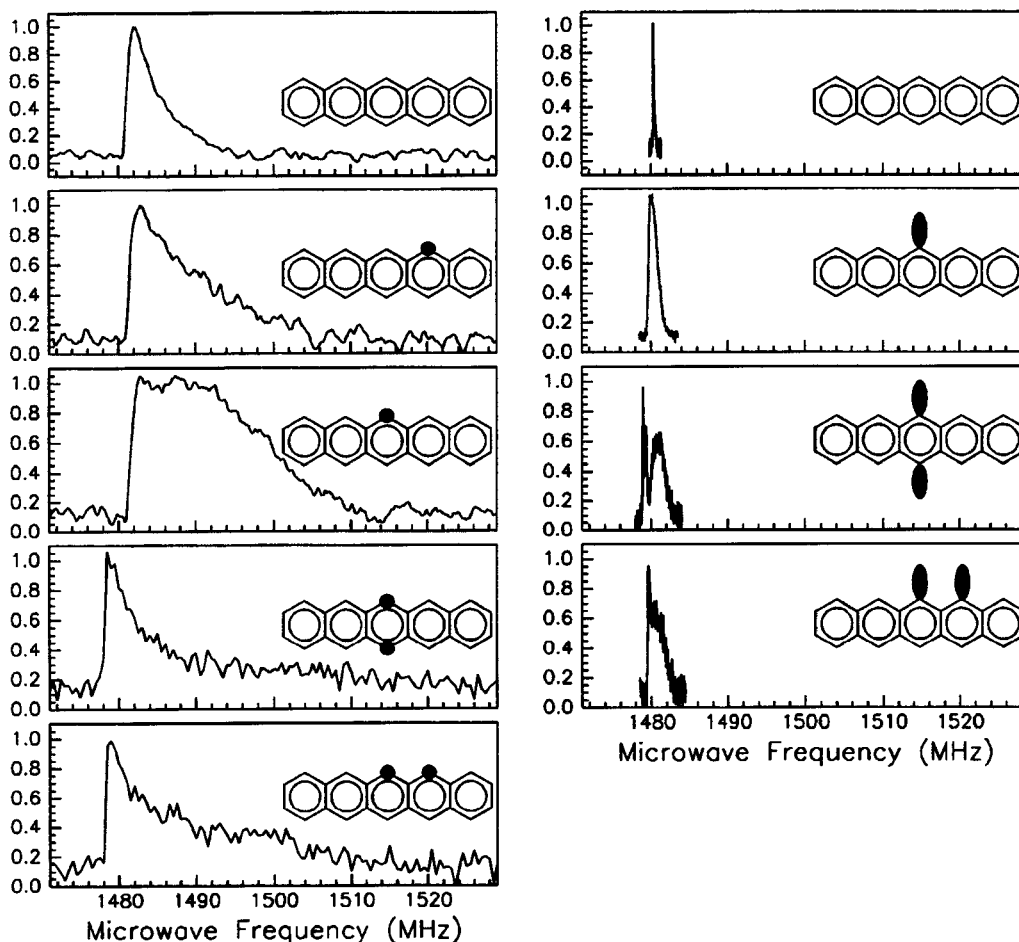


Figure 3. Fluorescence-detected T_x – T_z transitions of optically selected pentacene isotopomers. For ease of comparison the spectra have been normalized. The left-hand side of the figure features pentacene- h_{14} and pentacene- h_{14} molecules containing one or two ^{13}C nuclei at the positions marked by the black dots (from top to bottom, optical excitation of O_1 , satellites 5, 7, 15, and 13, in Figure 2a). The right-hand side of the figure shows pentacene- d_{14} and deuterated pentacene molecules containing ^1H nuclei at the positions marked by the black ellipses (from top to bottom, optical excitation of O_1 , satellites 3, 7, and 5, in Figure 2b). The difference between the line shapes of the FDMR spectra is not determined by saturation effects.

spectrum indicate to which origin, O_1 or O_2 , these satellites belong (vide infra).

For many of the spectral features in Figure 2, parts a and b, the corresponding FDMR spectra have been recorded. The laser was tuned into resonance with a particular line and microwaves were applied and swept through the T_x – T_z transition of pentacene. In Figure 3 a selection of FDMR spectra is shown. The left part of the figure shows FDMR spectra which were obtained for the natural-abundance sample. From top to bottom the optical excitation was in resonance with the O_1 zero-phonon line of $^{12}\text{C}_{22}^1\text{H}_{14}$, satellite 5 (equivalent FDMR spectrum for satellite 6), satellite 7, satellite 15, and satellite 13 (equivalent FDMR spectrum for satellite 14) in Figure 2a. The right part of the figure shows FDMR spectra obtained for the deuterated sample. From top to bottom the optical excitation was in resonance with the O_1 zero-phonon line of $^{12}\text{C}_{22}^2\text{H}_{14}$, satellite 3, satellite 7, and satellite 5 (equivalent FDMR spectrum for satellite 6) in Figure 2b. Obviously the line shape, both width and structure, of the magnetic-resonance transition varies strongly with the optical excitation frequency for both samples.

Discussion

As Figure 2 shows, high-resolution fluorescence-excitation spectra of high-quality mixed crystals of pentacene in *p*-terphenyl have enabled us to uncover spectral details that are

normally hidden under the inhomogeneously broadened $S_1 \leftarrow S_0$ zero-phonon line. Here we will argue that the satellites of the most intense zero-phonon line derive from isotopomers in which for pentacene ^{13}C replaces ^{12}C , and for pentacene- d_{14} ^1H replaces ^2H . In addition it will be shown that the corresponding FDMR spectra allow assignment of each specific line to a particular isotopomer.

The energy difference corresponding to the $S_1 \leftarrow S_0$ zero-phonon transition may be written as

$$\Delta E_{1-0} = E_{e1} + \frac{1}{2}h \sum_{i=1}^{3N-6} (\nu_i^{(1)} - \nu_i^{(0)}) \quad (1)$$

where E_{e1} reflects the purely electronic part and the summation corresponds to the difference in zero-point vibrational energy of the electronically excited and ground states. In general the vibrational frequencies of the molecule in the two electronic states will not be equal owing to changes in the molecular force field upon excitation. As a consequence the spectral position of the $S_1 \leftarrow S_0$ transition may depend, albeit slightly, on the isotopic composition. For a natural abundance sample a splitting of the spectral origin into several components is expected, with a relative intensity distribution that reflects the abundance of the various isotopomers. From the natural abundance of ^{13}C (1.1%) it follows that 19.2% of all pentacene molecules (22

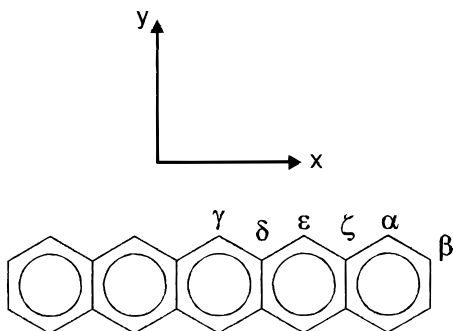


Figure 4. Schematic representation of the labeling scheme for the symmetry inequivalent carbon positions in pentacene. For the isolated molecule (D_{2h} symmetry as shown) one obtains a classification into one pair (γ) and five quartets (α , β , δ , ϵ , and ζ). Upon substitution into the *p*-terphenyl host crystal (site symmetry C_i) each quartet splits into two pairs of symmetry equivalent positions.

carbon atoms) contain a single ^{13}C atom. For a pentacene molecule of D_{2h} symmetry one expects, besides the main “all ^{12}C ” line, a pattern of six ^{13}C satellite lines with a mutual intensity ratio of $\alpha:\beta:\gamma:\delta:\epsilon:\zeta = 4:4:2:4:4:4$ (Figure 4). Previously we have shown that the set of satellites labeled 1–7 in Figure 2a must be attributed to molecules that contain a single ^{13}C atom, while the weaker features 8–15 in Figure 2a correspond to pentacene molecules that contain two ^{13}C atoms.^{7,8}

A single proton in a deuterated pentacene molecule shifts the zero-phonon line to the red by a few wavenumbers.⁹ Because this is of the same order of magnitude as the O_1/O_2 site separation, the spectrum for deuterated pentacene in Figure 2b becomes a complex superposition of O_1 - and O_2 -related patterns. For clarity we focus on those spectral features that belong to the O_1 origin, indicated by the numbers 1–11 in Figure 2b. These satellites originate from deuterated pentacene molecules that contain up to 4 residual protons. These protons most probably are bound to carbon nuclei in the ϵ or γ positions of pentacene (see Figure 4) because these positions are known to be chemically most reactive.¹⁰

To achieve an identification of the isotopic constitution of the molecules responsible for the various satellites two independent sources of information can be utilized: first, the spectral position of the zero-phonon line of an isotopomer with respect to the main line and, second, the FDMR spectra obtained with the laser in resonance with a particular isotopomer absorption. Prior work on naphthalene and anthracene indicated an empirical sum rule for ^{13}C isotope shifts.¹¹ It was found that the isotope shifts of bands for molecules containing two ^{13}C nuclei can be accurately predicted by taking the sum of the shifts observed for the corresponding mono- ^{13}C molecules. Our data lead us to infer that a similar relation holds true for ^1H induced shifts.

The identification of the isotopomers from the FDMR spectra is based on the position-specificity of the hyperfine interaction. The electron-spin density varies over the carbon atoms of pentacene, and the major contribution to the hyperfine interaction is given by the interaction between the electron-spin density on a carbon atom and the nuclear spin of that carbon and the

Table 1. A_{zz} Components of the Hyperfine Interaction Tensor for Hydrogen and Carbon Isotopes

nucleus	nuclear spin	A_{zz} (MHz)
^1H	$I = 1/2$	−61
^2H	$I = 1$	−11
^{13}C	$I = 1/2$	307

Table 2. Spin-Density Distribution of Pentacene in the Lowest Triplet State¹⁶

carbon position	spin density
β	0.025
α	0.045
ϵ	0.128
γ	0.188

connected ^1H or ^2H . The Hamiltonian that describes the hyperfine interaction can be written as

$$\hat{H}_{\text{HF}} = \sum_i \rho_i \hat{S} \cdot \vec{A}^{(i)} \cdot \hat{I}_i \quad (2)$$

where ρ_i denotes the triplet spin density at carbon nucleus i , or at the carbon position to which proton i is bound, $\vec{A}^{(i)}$ the hyperfine interaction tensor of nucleus i for $\rho_i = 1$, and \hat{S} and \hat{I}_i the electron spin angular momentum operator and the nuclear spin angular momentum operator of nucleus i . The sum runs over all nuclei of the molecule that carry a nuclear spin. For example, in a second-order perturbation treatment the energy shift of the zero-field triplet sublevels owing to the hyperfine interaction with a $I = 1/2$ nuclear spin may be approximated by¹²

$$\begin{aligned} \Delta E_x &\approx \frac{1}{4} \left| \sum_i (\pm \rho_i A_{zz}^{(i)}) \right|^2 / (E_x - E_y) \\ \Delta E_y &\approx \frac{1}{4} \left| \sum_i (\pm \rho_i A_{zz}^{(i)}) \right|^2 / (E_y - E_x) \\ \Delta E_z &= 0 \end{aligned} \quad (3)$$

These shifts result in a distribution of energies for the nuclear spin substates of each triplet sublevel which determines the shape of the magnetic-resonance line. Similar expressions apply for ^2H ($I = 1$) nuclei. From eq 3 it is obvious that the magnitude of both the hyperfine-tensor element A_{zz} and the triplet spin density determines the width of the magnetic resonance line. In Tables 1 and 2 the principal value A_{zz} (including both the isotropic and the anisotropic part) for ^1H , ^2H , and ^{13}C ^{13–15} and the triplet spin densities at the distinguishable carbon positions in pentacene¹⁶ are given. Inspection of the numbers in Tables 1 and 2 reveals that a ^{13}C nucleus in the ϵ or γ position of a pentacene molecule will broaden the triplet magnetic-resonance line most significantly. A similar situation arises for a perdeuterated pentacene molecule that contains a residual proton, bound to a carbon with a high triplet spin density. The nuclear magnetic moment of deuterium is only 15% of that of a proton, and owing to the quadratic nature of the hyperfine interaction

(7) Köhler, J.; Brouwer, A. C. J.; Groenen, E. J. J.; Schmidt, J. *Chem. Phys. Lett.* **1994**, *228*, 47–52.

(8) Brouwer, A. C. J.; Köhler, J.; Groenen, E. J. J.; Schmidt, J. *J. Chem. Phys.* **1996**, *105*, 2212–2222.

(9) Corval, A.; Krysch, C.; Astilean, S.; Trommsdorff, H. P. *J. Phys. Chem.* **1994**, *98*, 7376–7381.

(10) Corval, A.; Casalegno, R.; Astilean, S.; Trommsdorff, H. P. *J. Phys. Chem.* **1992**, *96*, 5393–5395.

(11) Doberer, U.; Port, H.; Rund, D.; Tuffensammer, W. *Mol. Phys.* **1983**, *49*, 1167–1178.

(12) Hutchison, C. A.; Nicholas, J. V.; Scott, G. W. *J. Chem. Phys.* **1970**, *53*, 1906–1917.

(13) Carrington, A.; McLachlan, A. D. *Introduction to magnetic resonance*; Wiley & Sons: New York, 1979.

(14) McConnell, H. M.; Strathdee, J. *Mol. Phys.* **1959**, *2*, 129–138.

(15) Horsfield, A.; Morton, J. R.; Rowlands, J. R.; Whiffen, D. H. *Mol. Phys.* **1962**, *5*, 241–250.

(16) Lin, T. S.; Ong, J.-L.; Sloop, D. J.; Yu, H.-L. In *Pulsed EPR: a New Field of Applications*; Keijzers, C. P., Reijerse, E. J., Schmidt, J., Eds.; North-Holland: Amsterdam, 1989; pp 191–195.

Table 3. The Spectral Shifts and Assignments of the Satellites for the Natural Abundance Sample^a

satellite	blue shift (cm ⁻¹)	calcd (cm ⁻¹)	assignment of the ¹³ C position
1	0.056		β
2	0.114		ζ
3	0.292		$(\alpha/\delta)_1$
4	0.337		$(\alpha/\delta)_2$
5	0.493		ϵ_1 (*)
6	0.515		ϵ_2 (*)
7	0.659		γ (*)
8	0.778	0.773, 0.785	$\zeta + \gamma, (\alpha/\delta)_1 + \epsilon_1$
9	0.819	0.807	$(\alpha/\delta)_1 + \epsilon_2$
10	0.856	0.852	$(\alpha/\delta)_2 + \epsilon_2$
11	0.949	0.951	$(\alpha/\delta)_1 + \gamma$
12	1.007	1.008	$\epsilon_1 + \epsilon_2, (\alpha/\delta)_2 + \gamma$
13	1.155	1.152	$\epsilon_1 + \gamma$ (*)
14	1.180	1.174	$\epsilon_2 + \gamma$ (*)
15	1.320	1.318	$\gamma + \gamma$ (*)

^a The numbering of the satellites corresponds to the numbers given above the spectrum in Figure 2a. The shifts are given with respect to the main line located at 16 882.739 cm⁻¹. In the assignment column the subscript distinguishes the two nonequivalent α , δ , and ϵ positions in pentacene, respectively. The calculated values have been obtained by summing the shifts of the respective mono-¹³C isotopomers. Assignments that are marked with an asterisk have been derived from FDMR, cf. Figure 3.

Table 4. The Spectral Shifts and Assignments of the Satellites for the Deuterated Sample^a

satellite	red shift (cm ⁻¹)	calcd (cm ⁻¹)	assignment of the ¹ H position
1	3.256		H ϵ_1
2	3.482		H ϵ_2
3	4.178		H γ (*)
4	6.732	6.738	H ϵ_1 + H ϵ_2
5	7.442	7.434	H γ + H ϵ_1 (*)
6	7.662	7.660	H γ + H ϵ_2 (*)
7	8.342	8.356	H γ + H γ (*)
8	10.982	10.916	H γ + H ϵ_1 + H ϵ_2
9	11.609	11.612	H γ + H γ + H ϵ_1
10	11.809	11.838	H γ + H γ + H ϵ_2
11	15.099	15.094	H γ + H γ + H ϵ_1 + H ϵ_2

^a The numbering of the satellites corresponds to the numbers given above the spectrum in Figure 2b for O₁. The shifts are given with respect to the O₁ main line located at 16 915.629 cm⁻¹. In the assignment column the subscript refers to the carbon position to which the proton is bound, where ϵ_1 and ϵ_2 distinguish the two nonequivalent ϵ positions in pentacene (here the positions ϵ_1 and ϵ_2 correlate either with ϵ_1 and ϵ_2 from Table 3 or with ϵ_2 and ϵ_1 , respectively). The calculated values have been obtained by summing the shifts of the respective mono-¹H isotopomers. Assignments that are marked with an asterisk have been derived from FDMR, cf. Figure 3.

in zero-field the line width of the triplet transition is reduced to 120 kHz (fwhm) for the fully deuterated molecules. Magnetic resonance spectra of molecules that contain one or more protons bound to a carbon in position ϵ or γ show an additional broadening and/or splitting compared to those of the perdeuterated molecules.

Through analysis of the FDMR line shapes along these lines, we have been able to ascribe satellite lines in Figure 2 to various isotopomers present in the pentacene samples. The spectral shift and the assignment of the satellite lines with respect to the corresponding main line are summarized in Table 3 for the natural abundance sample and in Table 4 for the deuterated one. Two inequivalent ϵ positions are distinguishable, referred to as ϵ_1 and ϵ_2 , which points to a (slight) deviation of the pentacene geometry from *D*_{2h} symmetry, retaining inversion symmetry, upon substitution into the *p*-terphenyl crystal. For the natural abundance sample, Table 3, satellites 5(6) and 7 as well as 13-(14) and 15 can be unambiguously identified to originate from pentacene molecules with one or two ¹³C atoms in the ϵ and/or

γ positions on the basis of the corresponding FDMR broadening. Additional support for the assignment of satellites 13(14) and 15 is obtained from their spectral shift with respect to the main line, which corresponds to the sum of the individual shifts of the corresponding single ¹³C-containing isotopomers. The FDMR line shapes observed for excitation in the satellite bands 1 to 4 are, within experimental error, indistinguishable from that for ¹²C₂₂¹H₁₄. We ascribe these satellites to pentacenes in which a ¹³C is present at positions α , β , δ or ζ because the spin density on these nuclei is so low that no observable broadening of the FDMR lines is expected. The observed blue shifts of the optical transition lead us to the assignment of these satellites given in Table 3 based on a comparison with data for naphthalene and anthracene.^{8,11} Satellites 8 to 12 derive from molecules that contain ¹³C in two of the positions α , β , δ , and ζ because the observed spectral shifts can be reproduced to within 0.01 cm⁻¹ as the sum of the shifts observed for satellites 1 to 4.

For the deuterated sample, Table 4, the positions of the residual protons are referred to for example by H γ if a proton bound to a carbon in one of the γ positions of pentacene is meant. The assignments of satellites 3 and 5 to 7 have been deduced from FDMR through an analysis of the hyperfine interaction of the proton nuclear spin with the triplet spin. Satellites 4 to 7, 8 to 10, and 11 correspond to deuterated pentacenes containing two, three, and four protons at specific positions, respectively. Nearly all of the satellites 4 to 11 show red-shifts that can be reproduced within 0.01 cm⁻¹ as a sum of shifts observed for satellites 1 to 3. For satellites 8 and 10 the relatively large difference between the calculated and the observed red-shift probably derives from the superposition of O₁ and O₂ related satellites in this spectral region. The assignment of the latter satellites is supported by the resemblance of the intensity pattern observed for satellites 4 to 6 and 8 to 10 in Figure 2. Such similarity is expected because the isotopomers responsible for satellites 4 to 6 and 8 to 10 differ by one proton in the γ position.

Conclusions

In a natural abundance sample of pentacene in *p*-terphenyl it has proven possible to optically select and identify various isotopomers of pentacene. For example, molecules containing ¹³C in both γ positions having a natural abundance of less than 0.01% have been recognized. Similarly, pentacene molecules that contain up to four residual protons have been observed for a "completely" deuterated sample.

In principle it is possible to apply further spectroscopic methods to those rare isotopomers. This should not be hampered by the detection sensitivity because it has been demonstrated that vibrationally resolved spectra,^{17,18} spin coherences,¹⁹ hyperfine splittings,²⁰ and nuclear magnetic resonance transitions²¹ are detectable even for single pentacene molecules. Together with the aforementioned selection and identification techniques this opens the possibility to study specific isotopomers of pentacene in detail without a tremendous synthetic effort.

(17) Tchenio, P.; Myers, A. B.; Moerner, W. E. *J. Phys. Chem.* **1993**, *97*, 2491–2493.

(18) Fleury, L.; Tamarat, P.; Lounis, B.; Bernard, J.; Orrit, M. *Chem. Phys. Lett.* **1995**, *236*, 87–95.

(19) Wrachtrup, J.; von Borczyskowski, C.; Bernard, J.; Brown, R.; Orrit, M. *Chem. Phys. Lett.* **1995**, *245*, 262–267.

(20) Köhler, J.; Brouwer, A. C. J.; Groenen, E. J. J.; Schmidt, J. *Science* **1995**, *268*, 1457–1460.

(21) Wrachtrup, J.; Gruber, A.; Fleury, L.; von Borczyskowski, C. *Chem. Phys. Lett.* **1997**, *267*, 179–185.

Experimental Section

Sample Preparation. Pentacene-doped *p*-terphenyl crystals are grown by co-sublimation in a home-built oven. The sublimation temperatures are controlled by pumping oil from two independent temperature-stabilized reservoirs ($\pm 0.5^\circ$) along the sublimation chambers. Typical sublimation temperatures are 60°C for pentacene and 170°C for *p*-terphenyl. The sublimation chamber is flushed with 100 mbar of nitrogen for thermal contact, and an air-cooled glass finger serves as sublimation substrate. After a day of growth, thin sublimation crystals with a pentacene concentration of about 10^{-7} – 10^{-8} mol of pentacene/mol of *p*-terphenyl and dimensions of about $3 \times 3 \text{ mm}^2$ and a thickness of a few micrometers are harvested. The pentacene- h_{14} material (Aldrich, P180-2, chemical purity 98 atom %) is used without further purification whereas zone-refined *p*-terphenyl- h_{14} was kindly provided by Dr. A. Krüger. The isotopic constitution of both agents corresponds to natural abundance.

For the deuterated samples, *p*-terphenyl- d_{14} was purchased from Aldrich (D 1718-51-0, chemical purity 98 atom %) and pentacene- d_{14} was prepared by Dr. H. Zimmermann and kindly provided by Prof. Dr. H.-M. Vieth. Both materials have been used without further purification.

Instrumentation and Experiments. The samples are excited by an argon-ion pumped (Spectra Physics, 1702) single-mode dye laser (Coherent, 599-21). The wavelength of the laser is determined through comparison with an iodine reference spectrum whose absolute accuracy is given to be 0.006 cm^{-1} .^{22,23} The relative calibration accuracy is better than 0.003 cm^{-1} . The samples are mounted in a bath cryostat and cooled to 1.2 K. Inside the cryostat the laser beam is focused onto the sample by a lens ($f = 10 \text{ mm}$) to a spot of about $5 \mu\text{m}$ in diameter. A

(22) Gerstenkorn, S.; Luc, P. *Atlas du spectre d'absorption de la molécule d'iode*; CNRS, Paris, 1978.

(23) Gerstenkorn, S.; Luc, P. *Rev. Phys. Appl.* **1979**, *14*, 791–794.

typical value for the laser power incident on the cryostat is 1 nW, which corresponds to 5 mW/cm^2 in the focus.

The fluorescence of the sample is collected via a parabolic mirror and focused onto the photocathode of a photomultiplier (EMI, 9558AM). To prevent the incident laser light from reaching the photomultiplier a red-pass filter (Schott, RG 630) is used, allowing only the Stokes-shifted fluorescence to be transmitted. The signals of the phototube were treated with conventional photon-counting electronics (EG&G, Ortec 1182).^{24,25}

During the FDMR experiments the crystal is also exposed to microwaves provided by a small loop close to the sample. The microwaves were generated by a sweep oscillator (HP, 8350 B), stabilized to within 5 kHz by a frequency counter (EIP, 371) and a software-feedback. The on-off modulated microwaves are stepped in frequency with a typical dwell time of 4 s and the signal corresponding to the difference in photons counted during the “microwave on” and the “microwave off” periods is accumulated.

Acknowledgment. We thank Dr. A. Krüger for providing zone-refined *p*-terphenyl and Dr. H. Zimmermann and Prof. Dr. H.-M. Vieth for providing pentacene- d_{14} . This work is supported by the Stichting voor Fundamenteel Onderzoek der Materie (FOM), with financial aid from the Nederlandse Organisatie voor Wetenschappelijk Onderzoek (NWO). J. Köhler is a fellow of the Heisenberg-program of the Deutsche Forschungsgemeinschaft (DFG).

JA9731581

(24) Ambrose, W. P.; Basché, T.; Moerner, W. E. *J. Chem. Phys.* **1991**, *95*, 7150–7163.

(25) van der Meer, H.; Disselhorst, J. A. J. M.; Köhler, J.; Brouwer, A. C. J.; Groenen, E. J. J.; Schmidt, J. *Rev. Sci. Instrum.* **1995**, *66*, 4853–4856.